

# Investigation of Squeezed Light with an Injection Locked Laser

Thomas W. Noel *REU program, College of William and Mary*

July 31, 2008

## Abstract

Quantum physics implies a certain unavoidable amount of noise due to quantum fluctuations. In optics this noise can interfere with precise measurements in communications by diminishing the attainable signal to noise ratio. For this reason, among others, creation of states of light with noise below the quantum noise limit is of interest. Vacuum states of the electromagnetic field initially have equal uncertainty in the amplitude and phase quadratures. Then Polarization Self Rotation (PSR) interactions of elliptically polarized light with Rb atoms change the distribution of uncertainty between the quadratures. This unequal distribution of uncertainty is the hallmark of a "squeezed state" and can be used to suppress noise in one quadrature below the quantum noise limit. An implementation of an injection-locked laser system and homodyne detection to investigate squeezing is discussed. The dependence of squeezing on temperature, laser power and beam diameter is considered.

## 1 Introduction

Though we all know about the limitations that the uncertainty principle implies about position in measurement, most people seldom, if ever, see those limitations in action. The uncertainty in position and momentum of a baseball, for example, does not seriously impact the baseball player. In optics, however, many measurements are limited only by shot noise, which is the noise limitation imposed by quantum mechanics. Since this limit can (and often is) reached in experiment, a method for reducing noise below the limit becomes practically useful. The research presented here involves a method for noise suppression using the interaction of light with atomic vapor.

## 2 Theory

### 2.1 Quantum Noise Limit

Heisenberg's uncertainty principle implies a limitation on the precision that is possible in measuring properties of a quantum system. This limitation is most commonly referenced with respect to momentum and position.

$$\Delta x \Delta p \geq \frac{\hbar}{2} \quad (1)$$

The uncertainty relation means that the more precisely a particle's position is measured the less is known about its momentum. But this phenomenon is not solely concerned with position and momentum, rather quantum mechanics tells us that a similar relation holds for any pair of non-commuting observables. In quantum optics there is a similar relation governing the amplitude and

phase of the electromagnetic field. An electromagnetic field traveling in the  $\hat{z}$  direction can be written in a general way as a sum of terms like the following:

$$\hat{E}(z, t) = E_0 \sin(kz - \omega t)\hat{p} \quad (2)$$

where  $E_0$  is the amplitude of the field,  $k$  is its wavenumber,  $\omega$  is its angular frequency and  $\hat{p}$  is its polarization direction. Then we can define the amplitude and phase quadratures as  $X1 \propto E_0 \cos \phi$  and  $X2 \propto E_0 \sin \phi$ , respectively. The uncertainty relation then relates the amplitude and phase quadratures.

$$(\Delta X1)(\Delta X2) \geq 1 \quad (3)$$

in some contrived units. Equation 3 implies that there is a fundamental limit on the achievable noise in measurements of the amplitude or phase of light. Many light sources, including lasers, result in light with uncertainty evenly distributed between the quadratures. For such a light source the lower limit for noise in the amplitude or phase quadrature is given by  $\Delta X1 = \Delta X2 = 1$ . Any sufficiently precise measurement in optics will encounter this limit. However, since the uncertainty relation only guarantees that the product  $(\Delta X1)(\Delta X2)$  can not be less than one, either  $\Delta X1$  OR  $\Delta X2$  may be suppressed below one as long as the other increases to compensate. Thus, we may,

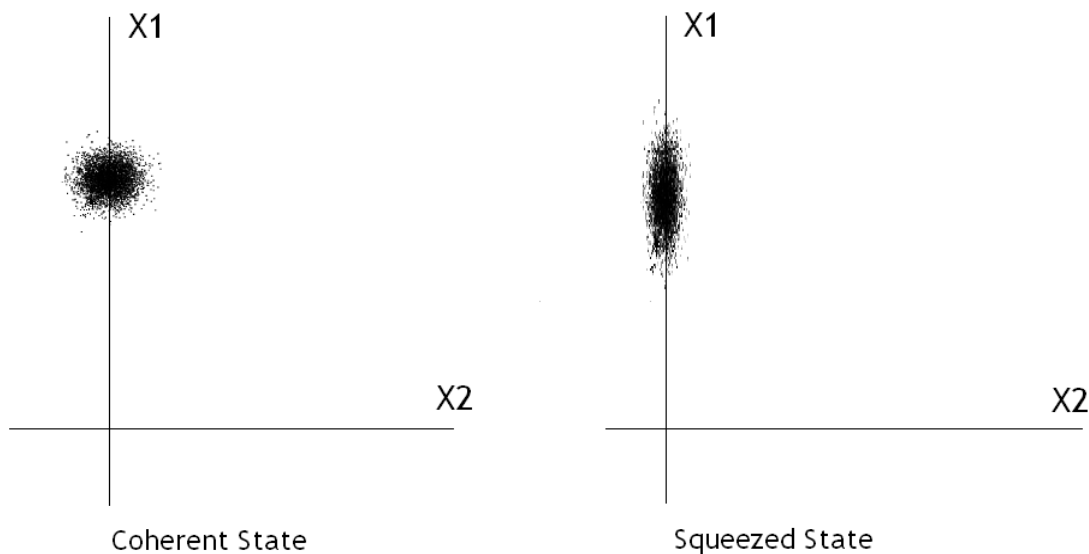


Figure 1: Coherent light (laser light) has equal uncertainty in both X1 and X2 so its forms a circular disk in the X1,X2 plane. The squeezed state shown here has suppressed uncertainty in X2 and correspondingly increased uncertainty in X1.

in theory, get very low noise in the amplitude quadrature, provided that we do not mind increased noise in the phase quadrature. Light with this property (different amounts of uncertainty in the amplitude and phase quadratures, with the uncertainty product equaling one) is called "squeezed light." Figure 1 shows a representation of such a squeezed state along with the so-called coherent light that approximates the output of lasers. If you imagine sampling photons from a light source repeatedly, each time measuring the amplitude and phase quadratures and creating a scatter plot

with these points on the X1, X2 plane, that is what Fig. 1 is supposed to represent. In such an experiment the amount of spread in the measurements of each quadrature would be equal for a coherent state, thus we see the scatter plot forms a circle. This circle is squeezed into an ellipse for the squeezed state, since the spread in one quadrature is decreased while the spread in the other increases.

## 2.2 Applications of Squeezed Light

Squeezed light can be used in a variety of applications, including interferometry and measurements related to quantum information processing in atomic systems. The beamsplitter in an interferom-

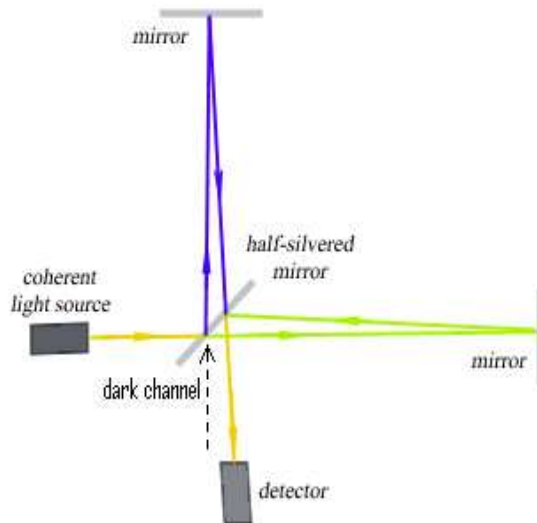


Figure 2: Interferometric measurements can benefit from squeezed light.

eter may only have light incident on one of the two input ports, while the other port is called the "dark channel" or "dark port." Even when there is no light intentionally shone on the dark port, vacuum field always enters. The vacuum fluctuations which couple into the dark port limit the attainable precision of the interferometer. Light squeezing gives us a method to reduce the amplitude of the vacuum fluctuations and thereby increase the level of precision of the interferometer. It has been suggested that light squeezing could help the Laser Interferometer Gravitational-wave Observatory (LIGO) to be able to see less dramatic gravitational shock-waves, to increase the frequency of occurrence of observable events. Another direction of application for light squeezing is in quantum information processing. In light storage and retrieval experiments, the amount of information stored could be increased by using squeezed light. The amount of information that can be encoded into a signal depends on the signal to noise ratio (SNR) of the system. The higher the SNR the more information can be encoded. One answer to this is to simply boost the strength of the signal. In some cases this will have a corresponding increase in noise power, and so will not be useful, and in all cases there is an upper limit to the power you can pump into the signal before some aspect of the system breaks down. In this limit, the only available way to increase

SNR is to suppress the noise in the system. This is where light squeezing can be of use. Since squeezed states can have suppressed noise in the relevant quadrature, they can be used to increase the amount of information encoded into the same total signal power. Since the light used in atomic quantum information processing experiments needs to interact with the atoms, the squeezed light would need to be tuned to the relevant atomic resonances in order to be useful in this application.

### 2.3 Squeezed State Creation

One method of squeezed state creation uses nonlinear crystals. In this method a pump field is shone on the crystal and a process called parametric down conversion converts photons from the pump field into two or more photons with lower frequencies. In the process statistical correlations in the created photons lead to the squeezed state. This method has been shown to produce squeezed states with up to 10 dB of noise suppression compared to a coherent state. However, squeezing with nonlinear crystals also has drawbacks. One is the complexity inherent in the squeezing apparatus involved. Also, in terms of the application to quantum information processing in atomic systems, there is a limit to the frequency of the squeezed light produced by crystals. Since the pump field must be twice the frequency of the output squeezed field, if we want squeezed light at atomic resonant frequencies the pump field may need to be in the near UV. Manipulating UV light with optical elements is a difficult task. More importantly, crystals become absorptive at UV frequencies and can be destroyed in the process. Therefore, the method of squeezing in atomic vapor is of interest, although it has not been shown to be as effective in terms of level of noise suppression yet. First proposed by A.B. Matsko, et al. in 2002, squeezing in atomic vapor very naturally allows the frequency of the squeezed light to be that of atomic resonances. When elliptically polarized light at an atomic resonant frequency is incident on atomic vapor, its polarization direction will rotate. This phenomenon is called Polarization Self Rotation (PSR). Fig. 3 gives a cartoon representation of PSR and defines  $\phi_{SR}$  as the self-rotation angle through which the polarization ellipse rotates. Although PSR will theoretically occur at any atomic resonance, I will consider the case of the D1 line of Rb since this is the resonance I used in my experimental studies. After undergoing PSR correlations between noise in the amplitude and phase quadratures cause the light the orthogonal polarization to be squeezed, with the magnitude of the squeezing increasing with the self-rotation angle. This will happen even if the only light in the orthogonal polarization incident on the Rb vapor is the vacuum field. In this case the result is a squeezed vacuum field.

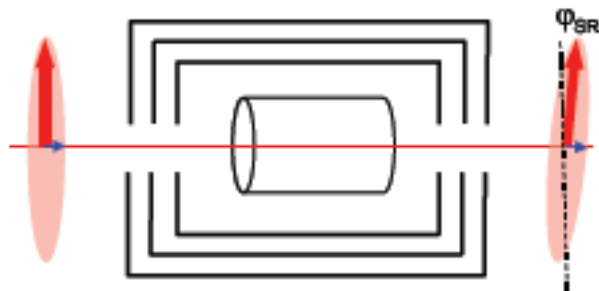


Figure 3: Elliptically polarized light incident on Rb vapor will undergo Polarization Self Rotation.

### 3 Experimental Setup

Our apparatus consists of four parts: an injection-locked laser, optics for shaping and directing the beam into the Rb cell, a homodyne detector, electronics for reading out and locking to the signal. The setup is fairly simple and does not require any very expensive optical elements, one advantage of this setup over crystal-based squeezing apparatus.

#### 3.1 Injection Locked Laser

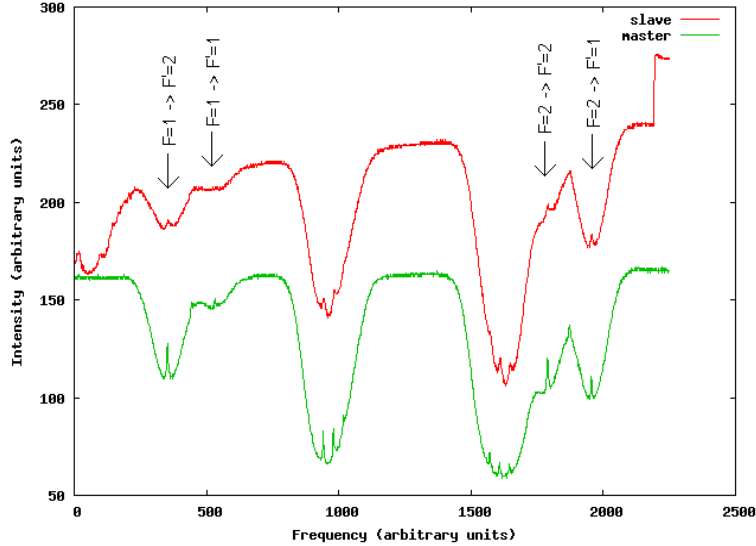


Figure 4: The injection lock is tunable over the frequency range of the Rb87 D1 line

Injection locking is a method of optical amplification. The output of a high-quality, low-power laser (master) is coupled into the cavity of a low-quality, high-power laser (slave). The slave then lases with the same high quality as the master, but with its potential for large output power. The quality of the lock depends strongly on matching the gain lines of the master and the slave. In general the slave laser will not lase at the same frequency as the master. If the difference between the frequency of the slave output and the master output is large then the slave laser will ignore the seed from the master and will output light in its natural mode. However, if the slave's light is near enough to the master in frequency then the slave will output light in the same mode as the master. It is therefore necessary to tune the slave's output to be similar in frequency to the master. Since the frequency of a laser diode is strongly dependent on the temperature of the diode, controlling the temperature of the diode makes it possible to carefully tune the frequency of the slave laser until it matches that of the master. In order to verify that my injection lock was good enough, we first shone the master laser onto a vapor cell containing both Rb85 and Rb87. After the light went through the cell we measured its intensity on a photodiode. When we sweep the master laser's output in frequency through the range of the relevant Rb resonances we get the lower line in Fig. 5. Note that the transmission through the cell drops when the laser is tuned to one of the Rb resonances. The Rb87 D1 lines are marked and the unmarked resonances are those of

Rb85. We then seed the swept output of the master laser into the slave and measure the slave's output after interaction with the same Rb cell. This yields the top line in Fig. 5. Note that the scales on the axes are arbitrary and the vertical separation of the two lines is artificial, for clarity. The two lines match very well through all the relevant resonances of the Rb87 D1 lines, but the slave's behavior becomes different than the master at each frequency extreme. This is called mode-hopping. The slave laser is not following the master's input at those frequencies. The tunability of the injection lock refers to the frequency range over which the slave follows the master, without any mode-hopping. Since the difference in frequency between the extremes of the D1 line are about 7 GHz apart, the tunability of this injection lock is about 7 GHz.

### 3.2 Shaping and Directing the Beam

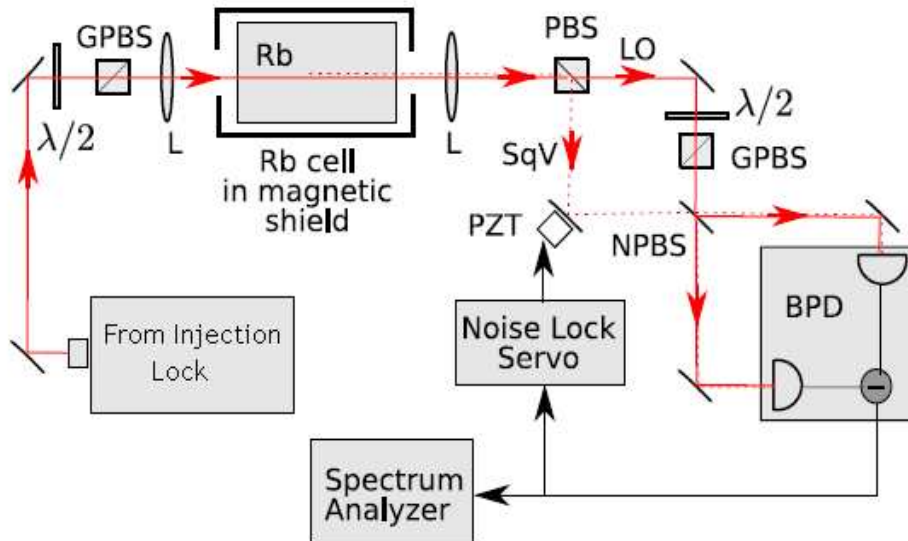


Figure 5: Schematic of the experimental apparatus

The experimental setup downstream of the injection locking system is shown in Fig. 5. The slave laser beam is focused into a cylindrical glass cell containing Rb87 (depending on the experiment at hand this cell may or may not contain Ne as a buffer gas, this will be noted when results are considered) with a pair of lenses (L). The minimum beam diameter inside the cell is  $.049 \pm .002$  mm FWHM. The cell is mounted in three-layer magnetic shield to minimize stray magnetic fields. Before entering the cell the laser beam passed through a high-quality Glan polarizing beam splitter (GPBS) to purify its linear polarization. A half-wave plate ( $\lambda/2$ ) placed in front of the GPBS allowed for smooth adjustment of the pump field intensity incident on the cell. After the cell the electromagnetic field in the orthogonal polarization [squeezed vacuum field (SqV)] was separated on a polarization beam splitter (PBS) and its noise properties were analyzed using homodyne detection. The original pump field is now used as the local oscillator (LO) after it is brought to the same polarization as the squeezed vacuum field using another GPBS and half-wave plate combination. The phase difference between the squeezed vacuum and the local oscillator were controlled using

a piezoceramic transducer (PZT). We then mixed these two fields on a 50/50 non-polarizing beam splitter (NPBS), and directed the two beams to a homemade balanced photodetector (BPD).

### 3.3 Homodyne Detection

Optical homodyne detection is a method for analyzing weak signals. An example of a homodyne detector is given in Fig. 5. It consists of the non-polarizing beam splitter that the squeezed vacuum and local oscillator fields are mixed on and the balanced photodetector that receives the mixed beams. The outcome of the homodyne detection scheme is that the weak signal (in our case the squeezed vacuum field) is amplified by a factor of the local oscillator amplitude (which can be made as large as the photodetector can handle). To show that this is the case, assume that the local oscillator field is given by  $2E_{LO}$  and the squeezed vacuum field is given by  $2E_{sq} \exp i\phi$  where  $\phi$  is the phase difference between the two fields. Then the outputs of the two ports of the non-polarizing beamsplitter are

$$E_{sq} \exp i\phi + E_{LO} \quad \text{AND} \quad E_{sq} \exp i\phi - E_{LO} \quad (4)$$

where the minus sign in the second output is a result of the boundary conditions placed on the fields at the beam splitter surface by Maxwell's equations. Since photodetectors give a response proportional to the intensity incident on them, we must square the expressions in (4) to get the photodiode response.

$$E_{LO}^2 + E_{sq}^2 + 2E_{LO}E_{sq} \cos \phi \quad \text{AND} \quad E_{LO}^2 + E_{sq}^2 - 2E_{LO}E_{sq} \cos \phi \quad (5)$$

Which, upon subtraction of the photodiode responses, becomes

$$4E_{LO}E_{sq} \cos \phi \quad (6)$$

As promised, the signal out is proportional to the weak signal in amplified by the large amplitude of local oscillator. This result relies on the beam splitter being precisely 50/50. That is it must take each field, the squeezed vacuum and the local oscillator, and split them so that half of each field goes to each photodiode. Also, more implicitly, the effect relies on mode-matching of the two fields. Since they come from the same laser in our experiment, the spatial modes should match well, but they must still overlap well spatially for the interference effect to occur. Both the mode-matching and the 50/50 of the beam splitter require careful alignment of the optical elements involved.

### 3.4 Electronics: Reading Out the Noise Measurement

The signal out from the homodyne detection is first fed into a low-noise preamplifier. We use an SRS SR560 set to AC coupling, with a 10kHz high pass filter that has a roll-off of 12dB/octave. Depending on the signal level, we apply various levels of amplification (essentially, we use as much gain as the preamplifier can handle before it overloads). The amplified signal then is sent to an HP 8568B spectrum analyzer which picks out a single sideband frequency to the noise spectrum, usually 1.2MHz. The video out of the HP spectrum analyzer outputs a signal proportional to the level of the signal on its screen. This video out is sent to a lock-in amplifier, which we use to lock to the squeezed and anti-squeezed quadrature noise levels. The output of the lock-in is sent to the PZT, which then corrects the phase between the local oscillator and the squeezed vacuum. This forms a phase locked loop that allows the signal to be locked to the level of noise in one of

the quadratures. Once the signal is locked we either read out the noise level visually from the HP spectrum analyzer at some particular sideband frequency or we send the preamplified signal to an Agilent E4405B spectrum analyzer which we use to take squeezed noise as a function of sideband frequency over some bandwidth, usually from 100 kHz to 2 MHz.

I had some problems with getting lock-in amplifiers to function. Several lock-ins that were tried had some noise on the output that would upset their ability to lock to the squeezed (or anti-squeezed) quadrature. I will enumerate these problems here. The SR530 lock-in introduces noise at low frequencies, especially a noise peak at 16 kHz. The output is modulated at its reference local oscillator frequency, although this noise is attenuated for large time constants. The SR510 lock-in has 60 Hz modulation on its output, which will be especially disruptive for high sensitivity, low time constant applications. There are also some delta function spikes on the output of 5-10 mV amplitude. The PAR model 5101 lock-in has modulation of the output at the reference local oscillator frequency, which is up to 100 mV in amplitude for high gain, low time constant applications. It also has some delta function spikes on its output of approximately 10 mV in amplitude which do not come with any readily discernible frequency. The PAR model 128A lock-in has output modulated at its reference frequency, but this last information is based on recollection far after the fact. What is sure is that it would not work for our purposes. Lastly, the SR830 lock-in behaved wonderfully.

## 4 Results

### 4.1 Rb Vacuum Cell: No Buffer Gas

Recall from the theory section that the predicted squeezing increases with the magnitude of the self-rotation angle. To test this prediction, we measured the self-rotation angle in the Rb vacuum cell at each Rb87 resonance for various incident laser powers. The cell is a glass cylinder 75 mm in length and 22 mm in diameter with the end faces tilted at an angle of about  $10^\circ$  to avoid backward reflection. In the study of self-rotation, the cell was maintained at  $43^\circ\text{C}$ . The cell was placed so that the focus of the pump field was inside the cell about 1/3 inch in front of the center of the cell (this was as close to the center as we could get the focus, without moving some optics that were obstructing the Rb cell's magnetic shielding). We placed a quarter-wave plate just before the Rb cell (after the Glan polarizing beam splitter) to introduce some ellipticity,  $\epsilon \approx 8^\circ$  into the incident beam. We define the ellipticity to be the angle between the fast axis of the quarter-wave plate and the polarization direction of the pump field after the Glan polarizing beam splitter. Fig. 6 shows the results for pump frequencies near the  $F_g = 1 \rightarrow F_e = 1$  transition. The degree of the self-rotation is much larger at the  $F_g = 1 \rightarrow F_e = 1$  transition compared to the  $F_g = 1 \rightarrow F_e = 2$  transition. Also, the self-rotation as a function of pump power reaches a maximum for  $P \approx 4$  to  $8$  mW. This result predicts that the best squeezing at the  $F_g = 1 \rightarrow F_e = 1$  transition should be found at a pump power of about 4 mW. However, this prediction could be complicated by the different absorption at different pump powers. The absorption is largest for low powers owing to the increased optical pumping of atoms to states which do not interact strongly with the light as the pump power is increased. Near the  $F_g = 2 \rightarrow F_e = 2$  transition the story is similar, Fig. 7 shows that detuning vicinity. Again there appears to be an optimal pump power range (at these pump frequencies it lies around 2 to 8 mW) with self-rotation degrading for powers lower and higher than the optimal range. Again the absorption decreases for increasing pump power.



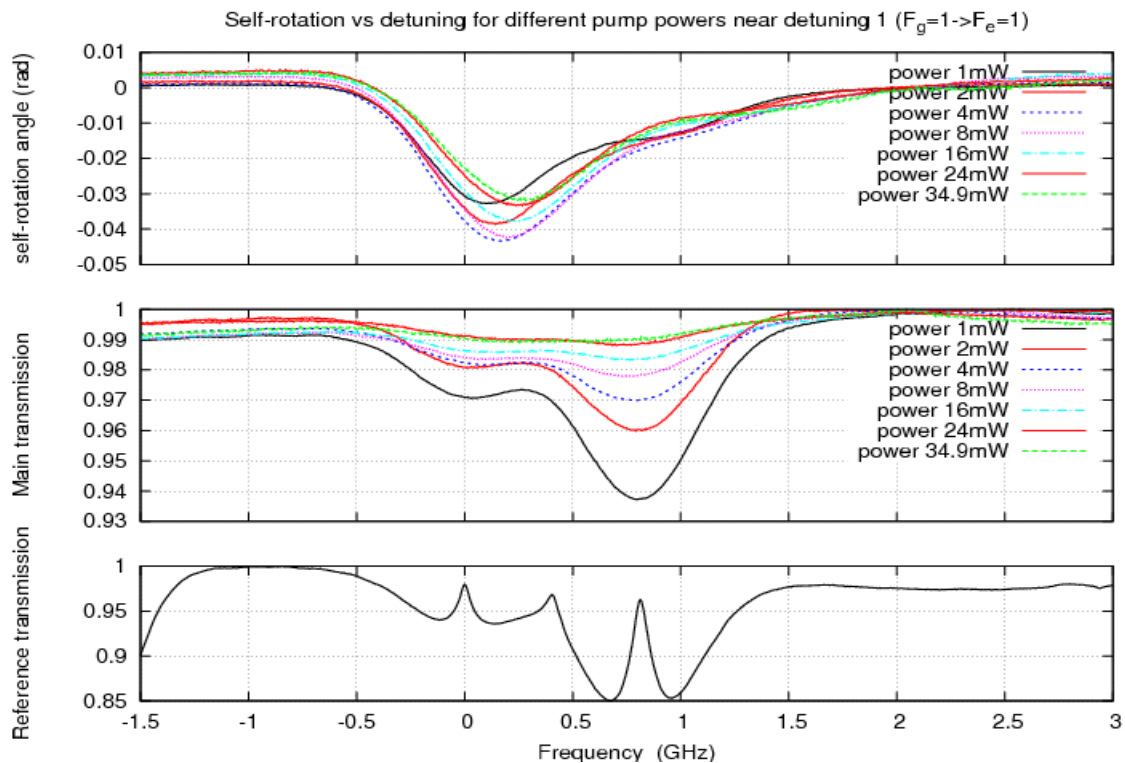


Figure 6: (Top) Polarization self-rotation angle ( $\phi_{SR}$ ) (Middle) Transmission through the main squeezing Rb87 cell (Bottom) Transmission through a reference Rb cell containing both Rb85 and Rb87. X-axis for each plot is the pump field frequency, with zero detuning corresponding to the  $F_g = 1 \rightarrow F_e = 1$  transition.

## 4.2 Squeezing Results in Rb Vacuum Cell

Since we did the self-rotation study at a specific temperature and focus of the beam in the Rb cell, let us first see what the power dependence of the squeezed noise is at this temperature and cell position. Measurement of these data points was done by visually reading off the difference between noise level when locked to the squeezed quadrature and shot noise level on an HP 8568B Spectrum Analyzer. I am confident that this method produces results that are good to  $\pm 1dB$ . I also measured the difference between the anti-squeezed quadrature and the squeezed quadrature (I call this difference the "contrast"), in the same way. This measurement is good to about  $\pm 2dB$ . Fig. 8 shows the results for squeezed noise and anti-squeezed noise for various pump powers at the cell parameters given earlier for the self-rotation study and for laser detuned to the  $F_g = 1 \rightarrow F_e = 1$  transition. The figure shows that the optimal power predicted by the self-rotation study does turn out to be optimal for minimizing the noise in the squeezed quadrature. Note, however, that the noise is at .2 dB with respect to shot noise. That is the "squeezed" noise is ABOVE shot noise. This is often the case for a significant part of the parameter space studied, and this extra noise will be discussed further later. We think that there is a source of noise coming from the atoms, and that this "atomic noise" is pushing the squeezed noise above shot noise level.

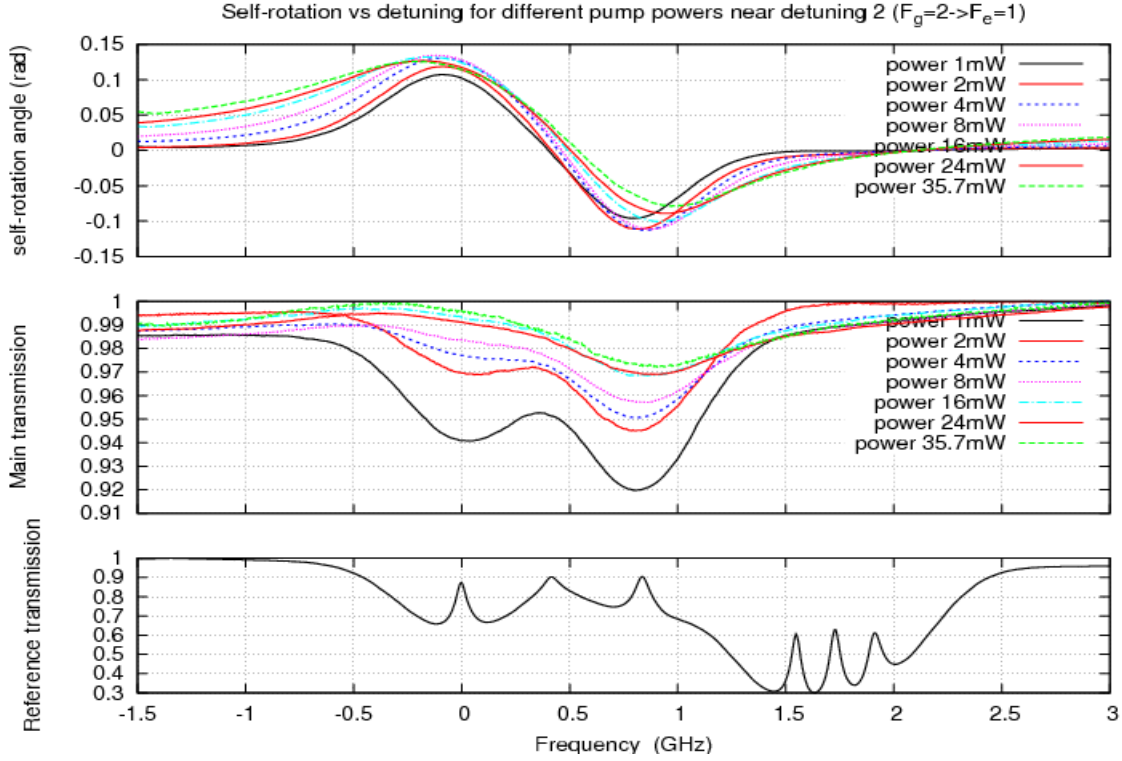


Figure 7: (Top) Polarization self-rotation angle ( $\phi_{SR}$ ) (Middle) Transmission through the main squeezing Rb87 cell (Bottom) Transmission through a reference Rb cell containing both Rb85 and Rb87. X-axis for each plot is the pump field frequency, with zero detuning corresponding to the  $F_g = 2 \rightarrow F_e = 1$  transition.

A systematic investigation of the dependence of squeezing on temperature and power at two different pump laser frequencies was done. The procedure was as follows. 1 Set the temperature of the Rb cell. 2 Set pump laser detuning to the vicinity of either  $F_g = 2 \rightarrow F_e = 2$  or  $F_g = 1 \rightarrow F_e = 1$  and search nearby frequency for best squeezing. 3 Set pump power to maximum. 4 Measure difference between shot noise and noise in locked squeezed quadrature. 5 Lock to anti-squeezed quadrature, measure difference between anti-squeezed noise and squeezed noise (contrast). 6 Set pump power to next level, bring shot noise back to same level as it was previously, repeat 4-6 until all power levels have been tested. 7 Set detuning to other place, repeat 3-6. 8 Set temperature to next point, repeat 2-7. For these measurements the squeezed and anti-squeezed noise levels were read visually off the HP spectrum analyzer, which was set to a center frequency of 1.2 MHz and zero span. The squeezing as a function of sideband frequency was checked from 100 kHz to 2 MHz and was flat for sideband frequencies over 600 kHz. Therefore the squeezed noise value at 1.2 MHz sideband frequency is a good representation of the broadband squeezed noise. This procedure was done for two different positions of the Rb vacuum cell in the pump field. One position was with the focus of the pump field near the center of the cell and corresponds to a smaller average beam diameter inside the cell. The other position was with the center of the cell one inch beyond the focus of the pump field and corresponds to a larger average beam diameter inside the cell. Results

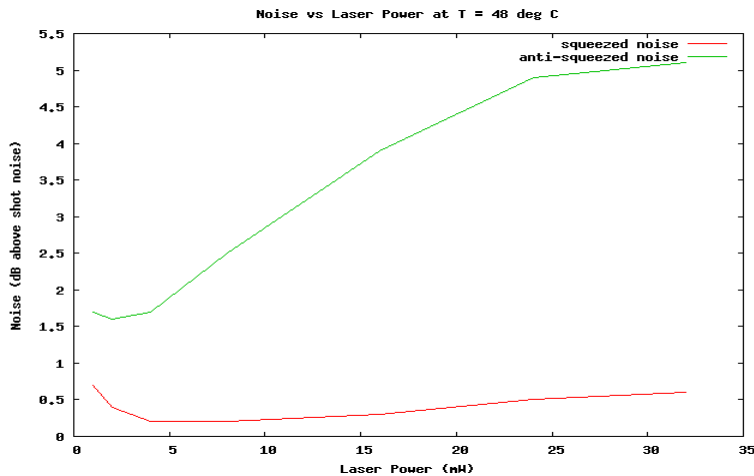


Figure 8: As predicted by study of self-rotation, the minimum noise is found at about 4 to 8 mW pump power.

from this procedure are plotted in various ways in the next several figures.

From Fig. 9 a couple of features can be recognized. First, squeezed noise is never below shot noise, although it reaches shot noise at the lowest temperature. Second, with respect to power there is a minimum for pump powers around 4 mW, again following the prediction of the self-rotation study.

Recall that contrast is defined as the difference between anti-squeezed noise level and squeezed noise level. Fig. 10 shows that as temperature or power decreased contrast decreased as well. Also note that the very low contrast near pump power of 4 mW and temperature of  $30^{\circ}\text{C}$  indicates that decreasing the temperature further would not have helped the squeezed noise in nearby parameters to reach below shot noise.

Fig. 11 is now looking at the noise in the squeezed quadrature when the pump field is tuned near the  $F_g = 2 \rightarrow F_e = 2$  transition. At this laser detuning there is some slightly different behavior. Now there are optimal points in both temperature and power with noise increasing if you move away in any direction. The optimal power is about 16 mW and the optimal temperature is  $41^{\circ}\text{C}$ . When both power and temperature are optimized a squeezing of  $\sim .1\text{dB}$  is observed.

At pump frequency corresponding to the  $F_g = 2 \rightarrow F_e = 2$  transition, Fig. 12 shows that the contrast behaves similarly to the other pump detuning studied. The contrast increases with temperature. As the power increases from 1 mW to 8 mW the contrast increases rapidly, but then only increases very slowly, if at all, as power is increased further.

Figs. 13-16 are plots of data taken when the Rb cell was placed so that its center was one inch beyond the focus of the pump field. In this position the average beam diameter is slightly larger than in the position where the focus is near the center of the cell. Fig. 13 shows that the squeezed noise generally follows the same trend with the pump field near the  $F_g = 1 \rightarrow F_e = 1$  transition as in the more focuses cell position. That is, the squeezed noise decreases as temperature decreases and reaches shot noise for low temperature. Also, though the trend is not as clear in this case, the optimal pump power appears to be 4 mW with the noise increasing as the power is raised or dropped from there.

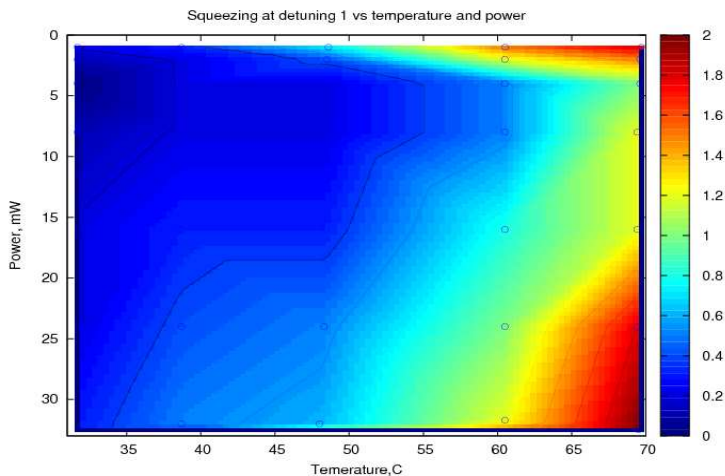


Figure 9: Squeezed noise as a function of pump power and cell temperature with pump field tuned near  $F_g = 1 \rightarrow F_e = 1$  transition and cell placed at the focus.

Fig. 14 shows that contrast decreases as temperature and power decrease, for pump detuning at the  $F_g = 1 \rightarrow F_e = 1$  transition with the cell one inch beyond the focus. This trend is the same as for the focused cell position.

Fig. 15 shows that the squeezed noise for pump detuning at the  $F_g = 2 \rightarrow F_e = 2$  transition with the cell one inch beyond the focus obeys the same qualitative trend as in the more focused case. Again there is an optimal point in both temperature and power. The optimal power is again about 16 mW, and the optimal temperature has increased to  $44^\circ\text{C}$ .

The behavior of contrast for pump detuning at the  $F_g = 2 \rightarrow F_e = 2$  transition with the cell one inch beyond the focus is complicated. The results are shown in Fig. 16. At low temperatures ( $< 40^\circ\text{C}$ ), the behavior appears to be the same as at the other cell position. This behavior entails swift contrast increase as power increases from 1 mW to 4 mW and then contrast is essentially independent of further power increase. However, for temperatures above  $40^\circ\text{C}$  the contrast seems to essentially be independent of power. This could reflect the same behavior as for lower temperatures, with the powers considered just not low enough to see the steep drop off in contrast.

### 4.3 Brief Comparison of Results for Different Pump Beam Diameter

### 4.4 Results of Squeezing in Rb Cell with Ne Buffer Gas

The following results concern squeezing in a Rb cell with 5 Torr of Ne as a buffer gas, intended to prolong the transit time of the Rb atoms inside the pump beam volume. The data was taken by locking to the squeezed quadrature, and looking at the squeezed noise as a function of sideband frequency for various pump powers. All data was taken at  $68^\circ\text{C}$ . When taking data on this cell I never varied the temperature, and since the best temperature for the vacuum cell was much lower, it is possible that even better noise suppression might be found at different temperature. Also, the beam was highly unfocused as it passed through the cell in the buffer gas cell case. The cell was placed about six inches before the focus of the pump field. All data for the buffered cell was taken

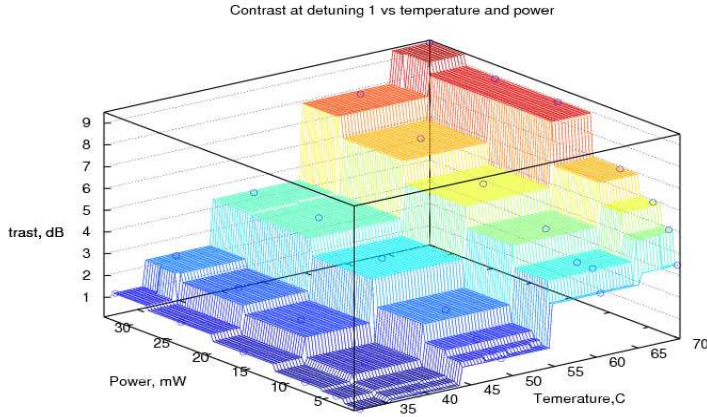


Figure 10: Contrast as a function of pump power and cell temperature with pump field tuned near  $F_g = 1 \rightarrow F_e = 1$  transition and cell placed at the focus.

with pump frequency corresponding to the  $F_g = 2 \rightarrow F_e = 1$  transition. Results for squeezed noise versus pump power for these parameters is shown in Fig. 17.

## 5 Conclusions

A consistent feature in the results shown here is that for most of the parameter space, no squeezing is seen. In fact, quite the opposite: for most parameters the interaction with the atoms is introducing additional noise. It is hypothesized that the atoms themselves are the source of the noise, that the noise is physical rather than technical. Given this, finding squeezing becomes a search for the optimal point between two (or more) forces. On the one hand, we want to maximize the amount of squeezing, but, on the other, we want to minimize the amount of atomic noise introduced. The interplay of these factors is what gives the results as a function of power, temperature, and other parameters its structure. In the future, it will be interesting to see a more clear study of how pump beam size affects the measured squeezing. Beam size involves two parameters, beam intensity and time of flight of Rb in the beam, both of which may be important. It will be exciting to see if polarization self-rotation squeezing in atomic systems can be optimized to the point where it will be useful in applications.

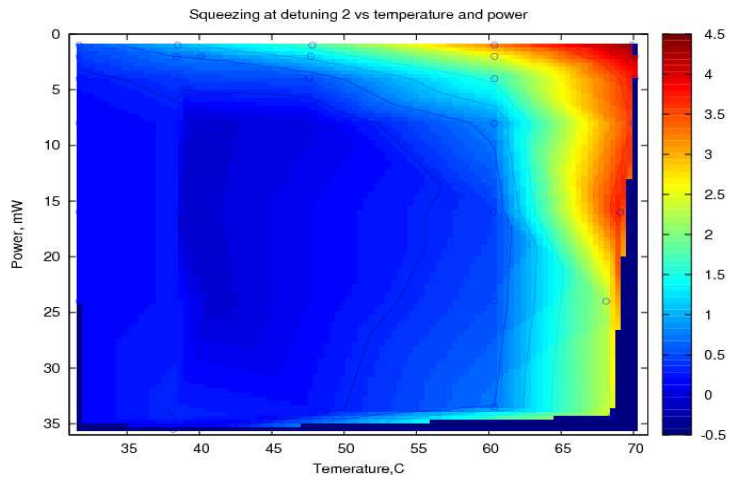


Figure 11: Squeezed noise as a function of pump power and cell temperature with pump field tuned near  $F_g = 2 \rightarrow F_e = 2$  transition and cell placed at the focus.

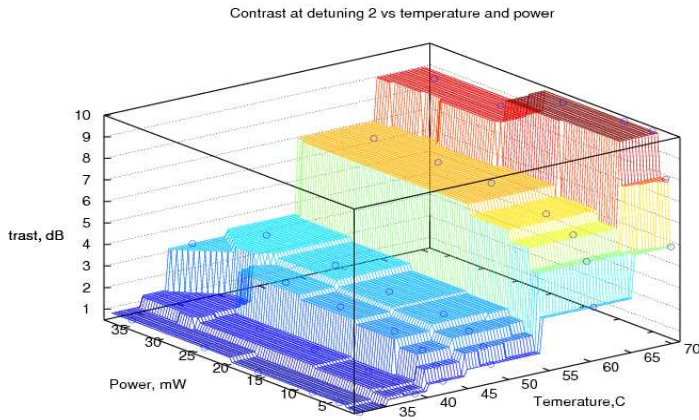


Figure 12: Contrast as a function of pump power and cell temperature with pump field tuned near  $F_g = 2 \rightarrow F_e = 2$  transition and cell placed at the focus.

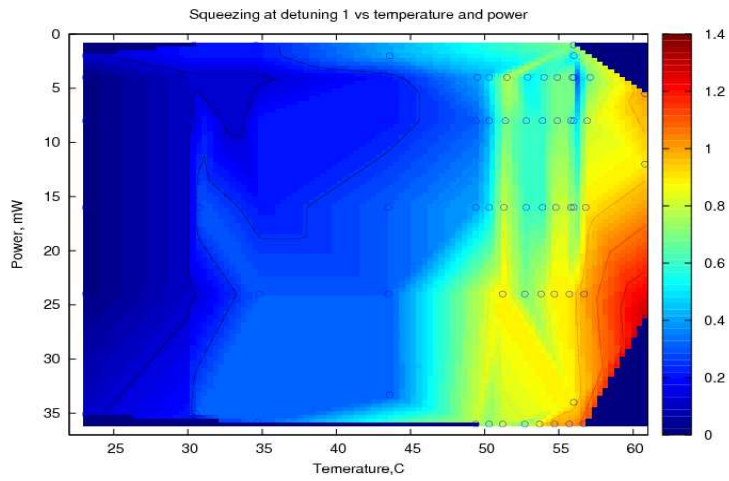


Figure 13: Squeezed noise as a function of pump power and cell temperature with pump field tuned near  $F_g = 1 \rightarrow F_e = 1$  transition and cell placed one inch beyond the focus.

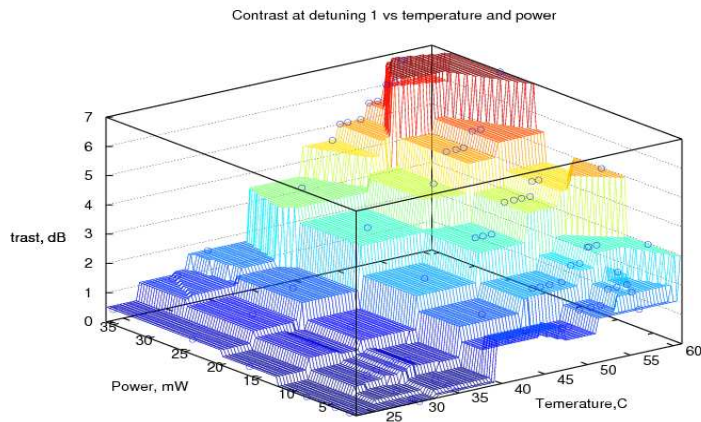


Figure 14: Contrast as a function of pump power and cell temperature with pump field tuned near  $F_g = 1 \rightarrow F_e = 1$  transition and cell placed one inch beyond the focus.

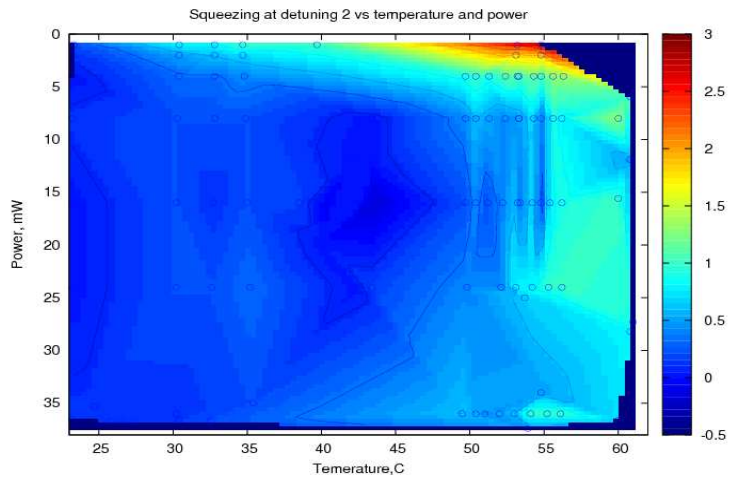


Figure 15: Squeezed noise as a function of pump power and cell temperature with pump field tuned near  $F_g = 2 \rightarrow F_e = 2$  transition and cell placed one inch beyond the focus.

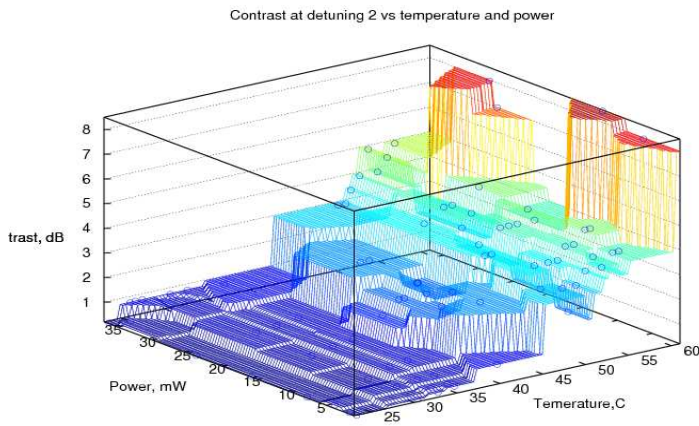


Figure 16: Contrast as a function of pump power and cell temperature with pump field tuned near  $F_g = 2 \rightarrow F_e = 2$  transition and cell placed one inch beyond the focus.



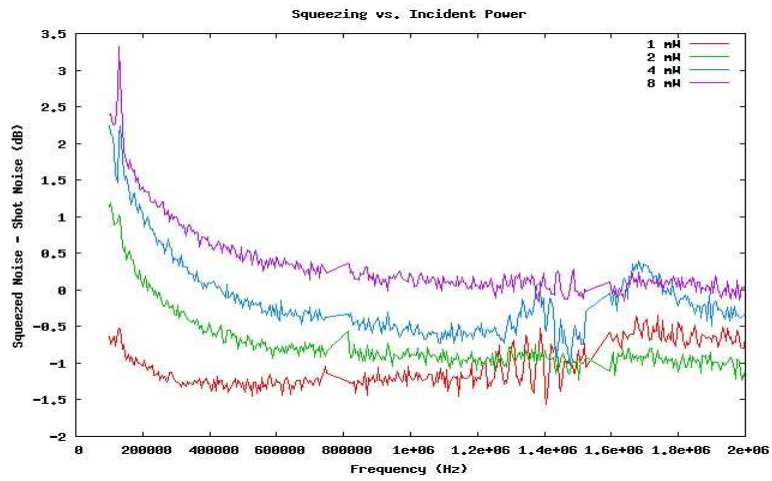


Figure 17: Squeezing as a function of sideband frequency for various pump powers with the pump frequency tuned near  $F_g = 2 \rightarrow F_e = 1$  transition and Rb cell with 5 T Ne buffer gas.